IOP Conf. Series: Materials Science and Engineering **371** (2018) 012056 doi:10.1088/1757-899X/371/1/012056

Empirical Stress Intensity Factor Equations for Cracked Steel Plates Repaired with Double-Sided FRP Patches

B Do[a] and A Lenwari[b]

Structural Engineering Division, Department of Civil Engineering, Faculty of Engineering, Chulalongkorn University, Bangkok THAILAND 10330
E-mail: [a]Bach.K@student.chula.ac.th, [b]Akhrawat.L@chula.ac.th

Abstract. This paper presents an approach that combines the finite element (FE) modeling and genetic programming (GP) to provide accurate empirical stress intensity factor (SIF) equations for center-cracked steel plates repaired with adhesive-bonded double-sided fiber-reinforced polymer (FRP) patches. Several past studies in recent years independently showed that the reduction on the SIF of cracked structures after the patch repair is dependent on many factors such as bonding techniques, material parameters, geometric parameters, environmental factors. In this study, the SIF of the repaired cracked steel plate was considered to be a function of seven parameters including the crack length, elastic modulus of FRP material, shear modulus of adhesive material, dimensions (width, length, and thickness) of rectangular FRP patches, and thickness of adhesive layers. Empirical SIF equations were created by the data mining process of genetic programming analyses performed on a database created from the FE results. The SIF values obtained from these equations were also compared with an analytical equation to assess whether their ability to perform well on a certain design or not. It was found that the proposed SIF equations fitted well with the FE results as the squared Pearson correlation coefficients R^2 are higher than 0.9. In addition, the correlations between proposed equations and the analytical equation are approximately 0.8.

1. Introduction

Fiber reinforced polymer (FRP) materials that consist of high strength fibers and tough resin matrix possess a lot of prominent and beneficial features such as high modulus and strength, low density, excellent fatigue resistance, great resistance to corrosion, and great flexibility [1]. In recent years, these features have become more attractive in structural engineering for strengthening structural members as well as for repairing cracked or defective ones.

Numerous previous studies showed that bonding of carbon fiber reinforced polymer (CFRP) patches strongly influences flexural strength of steel beams [2, 3], slightly increases lateral-torsional buckling capacity of steel girders [4], successfully opposes local buckling in steel hollow section members [5], and enhances the strength and the ductility of concrete-filled steel tubes [6]. The FRP bonding also increases flexural stiffness of repaired members [7] and reduces stresses in these members as transferred stresses to external components through adhesive shear stress [8]. In addition, it has been demonstrated that the crack-bridging effect from the adhesively CFRP patching [9] and the redistribution of stresses in a repaired structure cause a significant reduction on both the crack opening displacement and effective stress range at the crack tip [10]. The crack repair technique also shows the beneficial effects of increasing the fatigue performance and reducing the mode I of stress intensity factor (SIF) of cracked structures. Previous investigations showed that the repair technique can significantly increase the fatigue life of cracked steel beams from 50% to 4 times [4] and more than

Content from this work may be used under the terms of the Creative Commons Attribution 3.0 licence. Any further distribution of this work must maintain attribution to the author(s) and the title of the work, journal citation and DOI.
Published under licence by IOP Publishing Ltd

20% for cracked steel plates [11]. A significant reduction of the SIF due to the FRP patches was also reported for both cracked steel girders [12] and cracked steel plates [13].
The effectiveness of the repair design for a cracked structure is assessed based on the reduction of SIFs at the crack tip while adhesive shear stress and stresses in the FRP patch are within acceptable limits [10]. To facilitate the repair design, the closed-form SIF equation should be developed. However, the development of an accurate empirical closed-form SIF equation that incorporates the combined effects of several design parameters simultaneously is still a challenging work.
This paper presents an approach that combines the FE modeling and genetic programming (GP) to provide accurate empirical equations of the SIF in terms of the crack length, and six design parameters for a center-cracked steel plate repaired with adhesive-bonded double-sided FRP patches.

2. Rose's approach for the SIF solution

An important concept for a preliminary estimate of the SIF of a crack patching problem is the two-stage process proposed by Rose [14], as depicted in Figure 1. In the first stage, the un-cracked steel plate is assumed. The normal stress in the un-cracked steel plate underneath the patch, σ_s, is determined based on one-dimensional linear-elastic technique [15] as specified in equation (1). In the second stage, the steel plate is cut along a line segment as the central crack of length 2a. The stress $\sigma_0=\sigma_s(y=0)$ is applied internally as the pressure to the crack faces. The SIF for the crack configuration in stage II is determined by the well-known formula in equation (2).

$$\sigma_s(y)=2\left[\frac{\frac{\sigma_y t_s}{E_s t_s}}{t_s\left(\frac{1}{E_p t_p}+\frac{2}{E_s t_s}\right)}\right]\frac{\cosh(\lambda y)}{\cosh(0.5\lambda L_p)}+\frac{\frac{\sigma_y t_s}{E_p t_p}}{t_s\left(\frac{1}{E_p t_p}+\frac{2}{E_s t_s}\right)} \quad (1)$$

$$K=\sigma_s(y=0)(\pi a)^{1/2}\sqrt{\sec\frac{\pi a}{W_s}} \quad (2)$$

where

$$\lambda^2=\frac{G_a}{t_a}\left(\frac{1}{E_p t_p}+\frac{2}{E_s t_s}\right) \quad (3)$$

E_s, E_p, and G_a are the modulus of steel, the longitudinal modulus of FRP, and the in-plane shear modulus of adhesive, respectively; t_s, t_p, and t_a represent the thicknesses of the steel plate, FRP patch, and adhesive layer, respectively; σ_y is the uniform tensile stress at the steel plate ends; L_p is the length of the rectangular FRP patch.

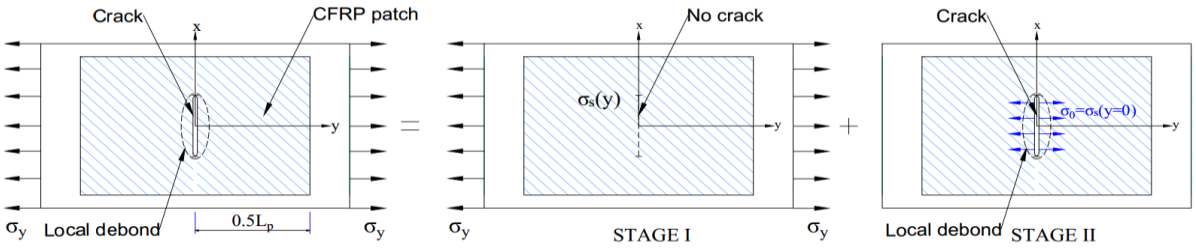

Figure 1. Two-stage analysis process for crack patching problem.

3. Finite element analyses

3.1. Geometric and material properties

To evaluate the average of the SIF value along the crack front of the repaired cracked steel plate, the three-dimensional FE analyses were performed using the general FE program ABAQUS/CAE. The subscript letters s, a, and p denote the steel plate, the adhesive layer and the FRP patch, respectively.
A total 175 FE models were generated for the steel plate with the length, L_s=500 mm, the width, W_s=90 mm, and the thickness, t_s=10 mm. As shown in Figure 2, the central crack of length, 2a, with a circular hole R = 5 mm was included. Different crack lengths of 20%, 30%, 40%, 50%, 60%, 70%, and 80% of the steel plate width were chosen.
The steel plate was subjected to a uniform pressure of σ_y=150 MPa on two ends. Due to symmetry about the two axes (i.e. the x-axis and the y-axis), a quarter model with symmetric constraints applied on the boundaries was used, as shown in Figure 3.

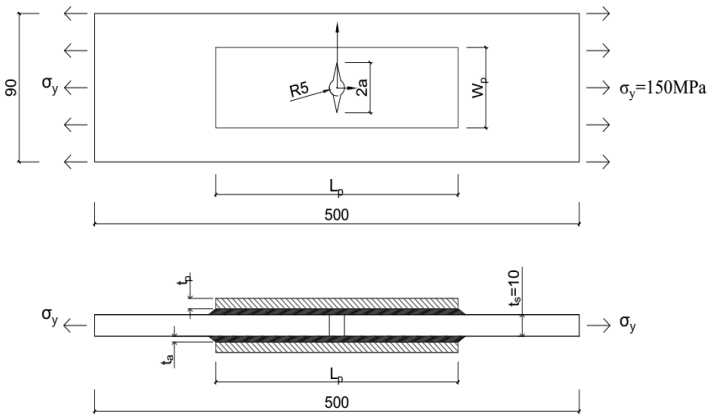

Figure 2. Geometry of cracked steel plate repaired with double-side FRP patches.

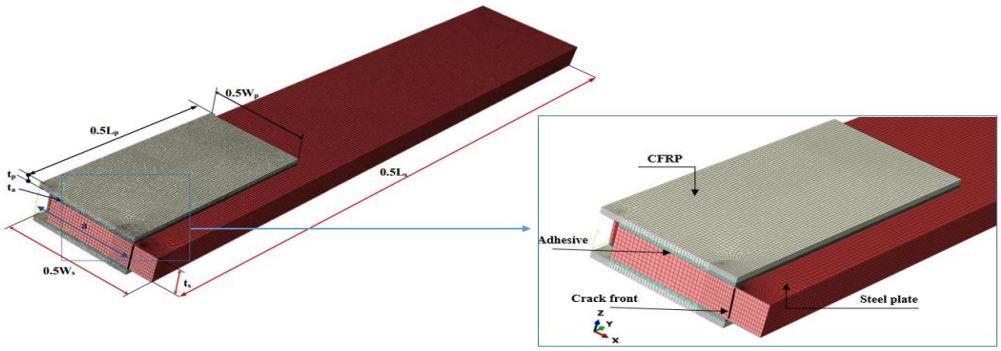

Figure 3. Quarter finite element model in ABAQUS.

The double-sided rectangular FRP patches and adhesive layers have the same dimensions: the length, L_p=L_a, and the width, W_p=W_a. The FE analyses were carried out for different geometrical configurations of L_p and W_p. The FRP patch width, W_p, was subdivided into five levels in the interval [2a, W_s] while five levels for the length of FRP patch, L_p, were 50, 100, 150, 200, 250 mm. For example, if the crack length was 2a=20%W_s=18 mm, the interval of W_p is [18, 90] and five levels for W_p were 18, 36, 54, 72, 90 mm.
The thickness of FRP plate, t_p, changed in the range from 1 to 1.8 mm with five levels, t_p={1, 1.2, 1.4, 1.6, 1.8}. The thickness of adhesive layers, t_a, varied from 0.25 to 1.25 mm with five levels, t_a={0.25, 0.50, 0.75, 1.00, 1.25}.
The material properties of the steel plate, five different FRP types and adhesive materials were adapted from a previous work [10], as given in Table 1. The mechanical behavior of all materials was linear elastic. Steel and adhesive were analyzed as linear isotropic elastic materials; the behavior of FRP material was orthotropic elastic in plane stress [16].

Table 1. Material properties of cracked steel plate, patches, and adhesives [10].

Materials	Material properties			
	Longitudinal modulus E_1 (GPa)	Transverse in-plane modulus E_2 (GPa)	In-plane shear modulus G_{12} (GPa)	Major in-plane Poison's ratio υ_{12}
Steel plate	200.00	n/a	76.92	0.30
FRP composite				
Boron/Epoxy 5505	219.90	21.40	6.89	0.21
Boron/Epoxy 5521	195.10	19.40	5.52	0.21
AS4/3501-6	124.10	11.00	5.52	0.34
IM6/SC1081	177.20	10.80	3.93	0.27
T300/F934	148.10	9.70	4.55	0.30
Adhesive				
FM-73	0.96	n/a	0.36	0.35
FM-300	1.29	n/a	0.46	0.40
FM-300K	1.37	n/a	0.52	0.32
A-9321	1.50	n/a	0.55	0.36
FM-36	1.81	n/a	0.67	0.35

3.2. Finite element models

A twenty-node quadratic brick element, C3D20, was used to represent steel and adhesive while a continuum shell element, SC8R, which allows for thick and thin shell applications, was used for FRP. To capture the singular stress and strain fields near the crack front, a collapsed three-dimensional element (collapsed C3D20) was assigned as steel elements near the crack front. All element types and their applications are clearly introduced in ABAQUS analysis user's manual [16]. The global size of steel plate elements was approximately 1 mm; the element size of 0.75 mm was used for both FRP and adhesive elements.

Furthermore, to construct an analysis matrix for performing FE analyses as well as to create a database for GP analyses, a total seven L-25 Taguchi arrays corresponding to 175 ABAQUS models were created. Each L-25 array with 25 observations was constructed based on the Taguchi methodology [17] for a particular crack length combined with the rest six design parameters; each parameter has five levels.

4. Genetic programming methodology

4.1. Genetic algorithm

Genetic algorithms (GAs) are iterative numerical algorithms for solving optimization problems motivated by natural selection and natural genetics [18]. Each GA operates on a population of candidate solutions represented by binary strings in a computer program; an example of numeric numbers encoded by binary strings is shown in Figure 4a.

Numeric values		Length-10 binary strings
30	encode →	**0 0 0 0 0 1 1 1 1 0**
60		**0 0 0 0 1 1 1 1 0 0**

a) GA individuals

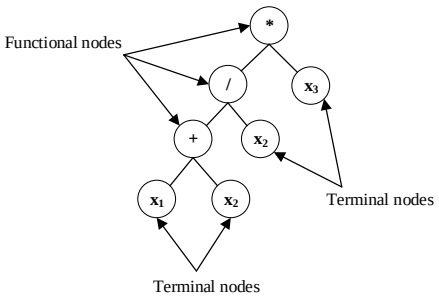

b) A GP individual $\left[\left(x_1 + x_2\right)/ x_2\right] x_3$

Figure 4. Example of candidate solutions in GA and GP.

At the start of each GA, randomly numeric values of independent variables in the solution space are encoded to corresponding computer strings in the computer program with respect to the 1-to-1 mapping property in which each binary string in coding space represents exactly one point in the numeric solution space and vice versa. GA then determines directly the fitness of each string, which is the value of a given objective function at each corresponding numeric point. After that, the algorithm scores all existing strings in the current computer program to determine which strings are good and which strings are weak. Based on this determination, good strings are combined randomly in pairs (crossover) while weak strings may change their own structure (mutation) to produce a better population of new strings for the next generation. This loop will be repeated until reaching stopping criterion as a given number of generations or iterations of the algorithm.

4.2. Genetic programming

Genetic programming (GP) is one important application of GA. The major difference between GP and GA is the representation of candidate solutions, which are binary strings in GA, as shown in Figure 4a and hierarchical computer programs (tree structures) in GP, as shown Figure 4b.

In the present study, GP maximized the objective function as the squared Pearson correlation coefficient R^2, which effectively measures the strength of a linear relationship between two sources obtained from FE models and obtained from GP models to provide the best fit models for the SIF. The main reason of this choice is that the SIF is affected by many factors; there is no evidence to decide what type of functional form to be defined first as the property of traditional regression techniques. In this case, GP property of simultaneously finding the model that most appropriately fits the data and corresponding numerical coefficients of the model, namely symbolic regression, is reasonably required.

The process of performing the GP includes three steps. In the first step, the initial population of a certain number of the tree structures is created by using materials from members of function (F) and terminal (T) sets. The F set includes arithmetic operations, mathematical functions, Boolean operations, conditional operators, or any user-defined functions [19]. Within a tree structure, each member of the F can occupy nodes that have two arguments, namely functional nodes. Meanwhile, the T set contains independent variable atoms or constant atoms [19]. These atoms may locate at terminal nodes, which have no explicit argument. Examples of the functional nodes and terminal nodes are given in Figure 4b. In the second step, GP computes R^2 values that represent the correlation between the FE results and those obtained from all tree structures in the current generation. Based on these R^2 values, GP stores all strings in a column vector and arranges them in a descending order of fitness value. After the arrangement, GP performs three genetic operators in a sequence: elite transfer (Figure 5a), crossover (Figure 5b), and mutation (Figure 5c). Finally, the last step defines the solution of the GP analysis that is the best-so-far tree structure. The GP's solution merely depends on the stopping condition of the GP analysis where the algorithm states the current population of tree structures and reports the best tree structure stored in the computer cache at the same time.

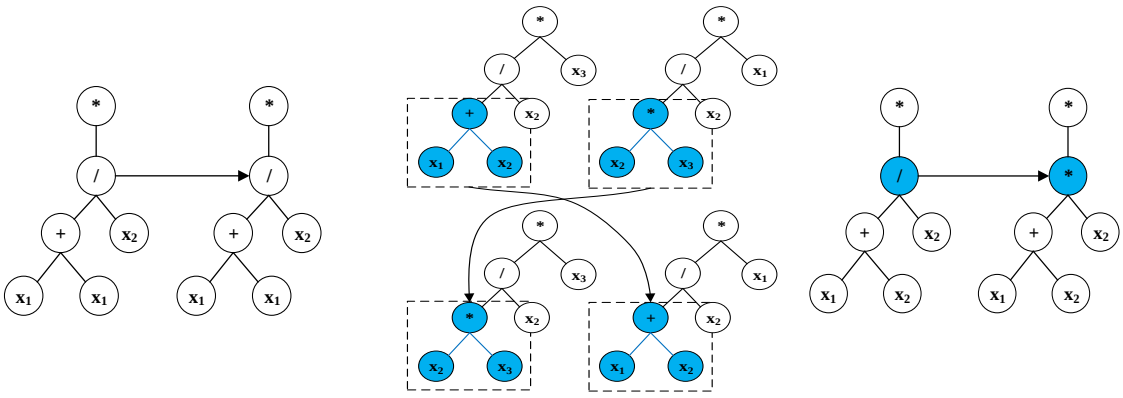

a) GP elite transfer b) GP crossover c) GP mutation

Figure 5. Example of three genetic operators of GP.

This study used HeuristicLab [20] as the GP tool for the SIF equations.

5. Results and discussions

5.1. GP Analyses

A database of 175 samples taken from FE results was randomly shuffled into seven different groups with 25 samples for each group, i.e., group A, B, C, D, E, F, and G to avoid the bias of the GP analysis on a certain group of samples. Corresponding to these groups, seven different models, i.e., M1, M2, M3, M4, M5, M6, and M7, were assigned. For example, in model M1, as given in Table 2, data group A was used for testing, and the rest six groups (B, C, D, E, F, and G) were used for training. This is consistent with the principle of separating the dataset in data mining where most of the data are assigned as a training set and a smaller portion is assigned as a testing set. The use of both the training set to produce an initial fitting model and testing this model by making predictions oppose the testing set provides a considerable significance to avoid overfitting of regression solution.

Table 2. Models used for GP analyses.

Model	Training set		Testing set	
	Data group	Number of data	Data group	Number of data
M1	B, C, D, E, F, G	150	A	25
M2	A, C, D, E, F, G	150	B	25
M3	A, B, D, E, F, G	150	C	25
M4	A, B, C, E, F, G	150	D	25
M5	A, B, C, D, F, G	150	E	25
M6	A, B, C, D, E, G	150	F	25
M7	A, B, C, D, E, F	150	G	25

All empirical equations were also developed with the same GP input of both function set F= {+, -, *, square, power} and terminal set T= {x_1, x_2…, x_7, [-5,5]}. Here, the constant atoms were in the interval [-5,5]. The stopping condition of each GP analysis was equal to the maximum number of generations of the algorithm loop, gen=500, 1000, 1500, and 2000. Additional control parameters defined at the beginning of each GP analysis are also provided in Table 3.

Table 3. Control parameters used in GP analyses.

Parameter	Value
Number of tree structures	10 000
Probability of mutation	25%
Elite count (reproduction option)	2
Maximum number of tree depth	10
Maximum number of tree length	50

5.2. Empirical stress intensity factor equations

The relationship between the SIF and seven parameters including the crack length, FRP modulus, FRP patch width, FRP patch length, FRP patch thickness, adhesive modulus, and adhesive layer thickness is characterized by the following mathematical model:

$$K = f\left(x_1, x_2, x_3, x_4, x_5, x_6, x_7\right)\sigma_y\left(\pi a\right)^{1/2} \tag{4}$$

where

$$x_1 = \frac{2a}{W_s}; x_2 = \frac{E_p}{E_s}; x_3 = \frac{W_p}{2a}; x_4 = \frac{L_p}{2a}; x_5 = \frac{t_p}{t_s}; x_6 = \frac{G_a}{E_s}; x_7 = \frac{t_a}{t_s} \tag{5}$$

Let, the GP analyses produced acceptable closed-form equations for the *f* factor when the corresponding coefficient R^2 is higher than 0.9.

Table ***4*** shows the coefficients R^2 of the three best models (M2, M3, and M7) obtained from a total of seven GP analyses for both training and testing sets. The scatter plots of Pearson correlation analyses of these models are also given in Figure 6a, b, and c. It can be clearly observed that after reaching the maximum number of generations as stopping criterion of the GP analyses, the R^2 values for training data of models M2, M3, and M7 are 0.941, 0.925, and 0.935, respectively. In
Table ***5***, the coefficients R^2 of the rest four models (M1, M4, M5, and M6) at gen=2000 are also almost 0.92. These results indicate a significantly high correlation between all GP models and FE results.

Table 4. Results of the best three GP analyses M2, M3, and M7 for f factor model.

gen	Model M2		Model M3		Model M7	
	Training set R^2	Testing set R^2	Training set R^2	Testing set R^2	Training set R^2	Testing set R^2
500	0.870	0.847	0.868	0.878	0.908	0.903
1000	0.890	0.900	0.904	0.940	0.928	0.892
1500	0.917	0.928	0.914	0.889	0.931	0.908
2000	0.941	0.901	0.925	0.947	0.935	0.900

Table 5. Comparison of seven f factor equation models.

Model	Gen	Training set, R^2	Testing set, R^2
M1	2000	0.921	0.857
M2	2000	0.941	0.901
M3	2000	0.925	0.947
M4	2000	0.916	0.907
M5	2000	0.916	0.934
M6	2000	0.916	0.912
M7	2000	0.935	0.900

In Figure 6d, the predicted *f* factor values of all seven proposed models are compared with the *f* factor values evaluated from FE results for the training samples and testing samples. It is recognized that proposed models are very similar even though they were built based on different data groups. Hence, it can be concluded that these models can have the same ability to provide a powerful tool for the prediction of the SIF for a cracked steel plate repaired by bonded double-sided FRP patches.
The closed-form SIF equation of model M2 with the highest coefficient R^2 for the training data (R^2=0.941) is expressed by:

$$K = \left[\left(f_1 + f_2 \right) f_3 + 0.9598 \right] \sigma_y \left(\pi a \right)^{1/2} \tag{6}$$

where

$$f_1 = c_0 x_5 \left[\left(c_1 x_7 \right)^{-1} + c_2 c_3 x_3 + c_4 x_4 + \left(c_5 x_1 \right)^{-2} + c_6 x_1 - 1.2218 \right] \tag{7}$$

$$f_2 = \left\{ c_7 c_8 x_3 \left[\left(c_9 x_7 \right)^{-1} - \left(c_{10} x_1 \right)^{5} - \left(c_{11} x_4 \right)^{-2} \right] - \left(c_{12} x_1 \right)^{-2} \right\} c_{13} x_7 \tag{8}$$

$$f_3 = c_{14} x_1 c_{15} x_2 c_{16} x_3 c_{17} \tag{9}$$

where c_0, c_1,…,c_{17} are constants, as given in Table 6.

Table 6. Coefficient values for SIF empirical equation provided by the GP model M2.

c_0	c_1	c_2	c_3	c_4	c_5	c_6	c_7	c_8
3.7443	2.4381	4.7712	1.3121	-0.5499	1.2800	1.7375	5.8520	1.2888
c_9	c_{10}	c_{11}	c_{12}	c_{13}	c_{14}	c_{15}	c_{16}	c_{17}
2.4381	1.7375	-0.5374	0.6311	1.1647	1.3527	0.3121	0.3193	-87.0620

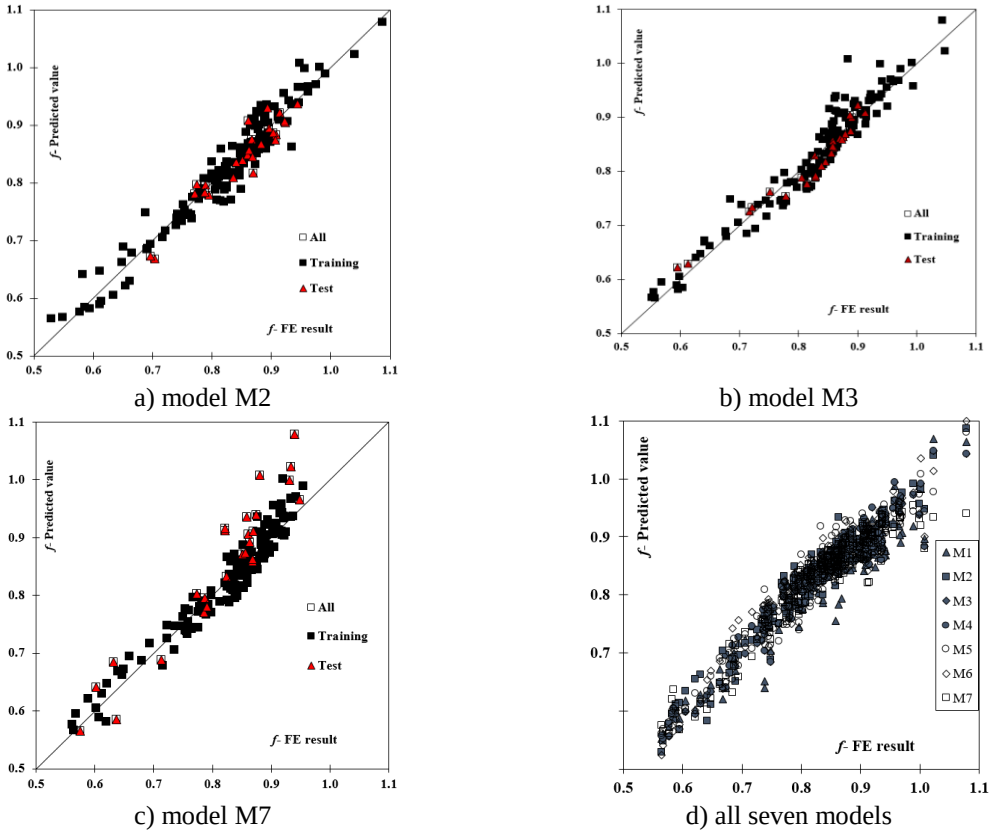

a) model M2 b) model M3

c) model M7 d) all seven models

Figure 6. Association for f factor from FE results and predicted values from a) model M2; b) model M3; c) model M7; d) all seven proposed models.

5.3. Comparison of the SIFs obtained from Empirical Equations and Rose's Approach

Recently, based largely on analyses derived from Rose's approach, some software programs were developed for the crack repair in the field of aerospace engineering [10]. This fact promotes the need for an evaluation of how well the analytical equation is represented by the proposed empirical equations. A comparison of the SIFs obtained from proposed equations and those obtained from Rose's approach in section 2 was made. It could be a good choice for checking the rationality of proposed models since so far, there have not been any equations that fully express the relation between the SIF and the stated seven design parameters. As the result, the SIFs obtained from proposed empirical equations are relatively smaller than the ones obtained from the analytical equation.

Furthermore, the correlation analyses used to assess the strength of the relationship between proposed equations and the analytical one were also performed. It was found that the correlations between the three best-proposed equations corresponding to the GP models M2, M3, and M7 and the analytical equation are 0.766, 0.761, and 0.770, respectively.

6. Conclusions

This paper is aimed at indicating the possibility of adapting the FE method combined with genetic programming to provide accurate empirical SIF equations for a cracked steel plate repaired with adhesive-bonded double-sided FRP patches. The results obtained from the numerical work led to the following conclusions:

- The SIF empirical equations obtained from GP analyses remarkable correlate with the FE models. The empirical equation that has the best correlation with FE results was also given.
- The SIFs predicted by the empirical equations are relatively smaller than those derived from Rose's approach. In other words, from a structural designer standpoint, each proposed equation is more economical than the analytical one.
- Relatively strong associations between proposed equations and the analytical equation are drawn as the correlations between them approach 0.8.

7. References

[1] A. Baker, "Bonded composite repair of fatigue-cracked primary aircraft structure," *Composite Structures,* vol. 47, no. 1, pp. 431-443, 1999/12/01/ 1999.

[2] A. Lenwari, T. Thepchatri, and P. Albrecht, "Flexural response of steel beams strengthened with partial-length CFRP plates," *Journal of Composites for Construction,* vol. 9, no. 4, pp. 296-303, 2005.

[3] A. Lenwari, T. Thepchatri, and P. Albrecht, "Debonding strength of steel beams strengthened with CFRP plates," *Journal of Composites for Construction,* vol. 10, no. 1, pp. 69-78, 2006.

[4] X.-L. Zhao, *FRP-strengthened metallic structures*. CRC Press, 2013.

[5] X.-L. Zhao and L. Zhang, "State-of-the-art review on FRP strengthened steel structures," *Engineering Structures,* vol. 29, no. 8, pp. 1808-1823, 2007.

[6] J. Teng, T. Yu, and D. Fernando, "Strengthening of steel structures with fiber-reinforced polymer composites," *Journal of Constructional Steel Research,* vol. 78, pp. 131-143, 2012.

[7] T. C. Miller, M. J. Chajes, D. R. Mertz, and J. N. Hastings, "Strengthening of a steel bridge girder using CFRP plates," *Journal of Bridge Engineering,* vol. 6, no. 6, pp. 514-522, 2001.

[8] J. Deng, M. M. Lee, and S. S. Moy, "Stress analysis of steel beams reinforced with a bonded CFRP plate," *Composite structures,* vol. 65, no. 2, pp. 205-215, 2004.

[9] C. Lin and P. Kao, "Effect of fiber bridging on the fatigue crack propagation in carbon fiber-reinforced aluminum laminates," *Materials Science and Engineering: A,* vol. 190, no. 1-2, pp. 65-73, 1995.

[10] C. N. Duong and C. H. Wang, *Composite repair: theory and design*. Elsevier, 2010.

[11] H. Liu, R. Al-Mahaidi, and X.-L. Zhao, "Experimental study of fatigue crack growth behaviour in adhesively reinforced steel structures," *Composite Structures,* vol. 90, no. 1, pp. 12-20, 2009/09/01/ 2009.

[12] A. Hmidan, Y. J. Kim, and S. Yazdani, *Stress Intensity Factors for Cracked Steel Girders Strengthened with CFRP Sheets*. 2014, p. 04014085.

[13] L. Gu, A. R. M. Kasavajhala, and S. Zhao, "Finite element analysis of cracks in aging aircraft structures with bonded composite-patch repairs," *Composites Part B: Engineering,* vol. 42, no. 3, pp. 505-510, 2011/04/01/ 2011.

[14] L. Rose, "Theoretical analysis of crack patching," *Bonded Repair of Aircraft Structures,* pp. 77-105, 1988.

[15] A. Albat and D. Romilly, "A direct linear-elastic analysis of double symmetric bonded joints and reinforcements," *Composites Science and Technology,* vol. 59, no. 7, pp. 1127-1137, 1999.

[16] U. s. M. Abaqus and E. U. s. Manuals, "Version 6.3, Hibbitt, Karlsson & Sorensen," *Inc. Rhode Island,* 2002.

[17] P. J. P. J. Ross, *Taguchi techniques for quality engineering: loss function, orthogonal experiments, parameter and tolerance design*. 1996.

[18] D. E. Goldberg, "Genetic algorithms in search, optimization, and machine learning, 1989," *Reading: Addison-Wesley,* 1989.

[19] J. R. Koza, *Genetic programming: on the programming of computers by means of natural selection*. MIT press, 1992.
[20] S. Wagner *et al.*, "Architecture and Design of the HeuristicLab Optimization Environment," in *Advanced Methods and Applications in Computational Intelligence*, R. Klempous, J. Nikodem, W. Jacak, and Z. Chaczko, Eds. Heidelberg %@ 978-3-319-01436-4: Springer International Publishing, 2014, pp. 197-261.

Acknowledgments
The authors gratefully acknowledge financial support for this study provided by the ASEAN University Network/Southeast Asia Engineering Education Development Network (AUN/SEED-Net).